INL/EXT-19-55962
Revision 0

Detailed Analysis of RUS Insertion Experiment and Scoping Studies for Performing Next Experiment using an Enriched Fuel Sample

Robert Schley, Larry Aagesen, Zilong Hua, and David Hurley

September 2019

The INL is a U.S. Department of Energy National Laboratory
operated by Battelle Energy Alliance

INL/EXT-19-55962
Revision 0

Detailed Analysis of RUS Insertion Experiment and Scoping Studies for Performing Next Experiment using an Enriched Fuel Sample

Robert Schley, Larry Aagesen, Zilong Hua, and David Hurley

September 2019

Idaho National Laboratory
Idaho Falls, Idaho 83415

http://www.inl.gov

Prepared for the
U.S. Department of Energy
Office of Nuclear Energy
Under DOE Idaho Operations Office
Contract DE-AC07-05ID14517

INTENTIONALLY BLANK

EXECUTIVE SUMMARY

Microstructure evolution due to irradiation in a nuclear reactor can have a dramatic effect on material properties. A better understanding of this evolution is necessary for developing improved nuclear fuels and materials. The ability to measure such changes in real time is extremely challenging due to high temperatures, high radiation fields, and limited access of the reactor environment. Through carefully designed experiments, measurement of elastic properties can be tied directly to microstructure. We present an instrument that has been developed to monitor in-pile changes in grain microstructure. The measurement approach involves optically exciting and detecting flexural waves in a thin cantilever beam. An instrument capsule based on this technique was fabricated and underwent an irradiation test in the TREAT reactor in May 2019. Analyses of the test results are presented in this report. Scoping studies on the expected impact of radiation on similar tests are also presented.

INTENTIONALLY BLANK

CONTENTS

FIGURES

INTENTIONALLY BLANK

Analysis of the RUS TREAT Experiment and Radiation Effects Scoping Study

1. INTRODUCTION

Microstructure evolution in nuclear fuel is governed by atomic transport facilitated by a highly non-equilibrium distribution of Frenkel defects (vacancy – interstitial pair). Over time in reactor, vacancies coalesce, forming small voids. Eventually, these voids are filled with fission gas. Transport of fission gas bubbles through the fuel plays a central role in eventual fuel failure. The interstitial portion of the Frenkel defect is preferentially drawn to dislocations, causing dislocations to multiply. The strain energy associated with dislocation production coupled with high temperatures causes profound changes to the grain microstructure. Grain restructuring or recrystallization occurs in both oxide and metallic fuel and can cause dramatic changes in material properties [1,2,3]. It has been shown that the elastic properties of materials are strongly influenced by porosity and grain microstructure [4].

In-pile monitoring of microstructure evolution of nuclear fuel would provide the computational materials science community direct access to a time-dependent, in-reactor environment. It would also enable monitoring in-pile material behavior that cannot be captured in a post-irradiation environment. This has motivated development of facilities that combine ion beam and electron beam irradiation with transmission electron microscopy [5]. However, creating neutron beams that have a flux and energy distribution representative of in-pile conditions is currently not possible, and thus, a comparable capability to examine the influence of neutron irradiation on microstructure evolution does not currently exist. Closing this capability gap will require development of innovative instruments that can indirectly measure changes in microstructure induced by neutron irradiation.

The work presented here describes the design and irradiation test of an in-pile laser resonant ultrasound spectroscopy method to measure changes in elastic properties caused by changes in microstructure. Using this approach changes in polycrystalline elastic properties are related to grain microstructure. In the test reported here, pure copper, preloaded with a well characterized microstructure, serves as a surrogate for more complicated metallic nuclear fuels. A highly textured grain microstructure was introduced into a copper sample by rolling. Then, the grain microstructure was monitored through the microstructure-induced elastic property changes of the sample as it underwent recrystallization. This optical fiber-based measurement technique involves optical excitation and detection of flexural vibrations in a thin cantilever. The device was designed to be compatible with the Material and Instrumentation Modular Irradiation Capability (MIMIC) which allowed simplified testing in the Transient Reactor Test (TREAT) Facility at Idaho National Laboratory (INL). Testing of the device in the reactor was conducted in May 2019. The results compared with laboratory tests, conducted at the INL Research Center (INL), are presented here along with scoping studies on the expected effects of irradiation.

2. MEASUREMENT APPROACH AND INSTRUMENT CAPSULE

2.1 Resonant Beam Vibrations

The approach for monitoring microstructure changes in-pile consists of repeatedly measuring the resonant frequency of a vibrating beam fabricated from the material of interest. Although laboratory-based implementation of this technique has been discussed in detail previously [6], the basic concept is presented here for completeness.

The natural frequency of vibrating beams has been widely used as a means of determining the elastic properties of materials, and numerous standards exist detailing such measurements [7,8,9]. For an isotropic material, the natural frequency depends only on the beam geometry, density, and elastic properties. Free-free beams are generally specified in these standards; however, cantilever beams offer

advantages for in-reactor measurements because the beams can be held rigidly in position and alignment with the detection system can be maintained.

Calculation of the natural frequency for flexural vibrations of a cantilever beam has been broadly discussed in the literature [10,11,12]. The simplest formulation is based on Bernoulli-Euler analysis which neglects shear deformation and rotational inertia. Calculation of the natural frequencies based on Bernoulli-Euler formulation can be performed using *Equation (1)* below [13]:

$$f_n = \frac{(\beta_n l)^2}{2\pi l^2}\sqrt{\frac{EI}{\rho A}}; \quad \text{with} \quad (\beta_1 l = 1.875,\ \beta_2 l = 4.694, \beta_3 l = 7.855, \dots) \tag{1}$$

where l is the beam length, E is the modulus of elasticity, I is the geometrical moment of inertia about the bending axis, ρ is the density, A is the cross sectional area, and $\beta_n l$ are solutions to the frequency equation for successive flexural modes with n being the mode number. While less accurate than other theories such as Timoshenko beam theory, this simple formulation gives accuracy to within 1-2% percent when $(n/l) * (I/A)^{1/2} < 0.01$ [14]. The instrument described below falls in this range such that the simple formulation is sufficient for monitoring elastic property changes in this case.

2.2 Detection Technique and Instrument Capsule

The instrument capsule uses optical methods for excitation and detection of the beam vibrations. Optical fibers are used to transmit the light to the sample. Figure 1 shows a cross section view of the test capsule along with an image of the assembled capsule prior to insertion in the reactor. The relationship of the cantilever beam and the fiber optic excitation and detection probes can be seen. Excitation is accomplished using an amplitude modulated laser. Excitation of the beam occurs through optical heating and the resulting thermal expansion. The laser modulation frequency is swept over a range that includes the first flexural mode of vibration. The data acquisition time for each frequency scan is approximately 40 seconds. Detection of the beam deflection is based on a fiber optic lever technique [15]. Detection light is delivered to the tip of the vibrating beam. Light exiting the optical fiber probe is reflected from the sample surface and coupled back into the fiber where it propagates back toward the source. The intensity of the light returning to the core of the optical fiber is dependent on the distance between the fiber tip and the sample, thus deflection of the cantilever beam causes an intensity modulation of the returning light. The returning light is delivered to a photoreceiver, whose output is processed and recorded as a function of modulation frequency by a lock-in amplifier. Because this detection method does not rely on the absolute light intensity, the measurement is only minimally affected by radiation-induced attenuation in the optical fiber – making it a good candidate for in-reactor measurements.

Development of a device for actual in-pile measurements required the design of an experiment capsule compatible with the test position in the TREAT reactor. The primary functions of the capsule include first, the ability to precisely clamp the cantilever beam in position, and second, to hold the optical fiber probes which deliver the light to excite and detect the beam vibrations. The capsule was fabricated from a 1.45 in. diameter titanium bar and consists of upper and lower halves. Titanium was used to minimize radioactive activation and for its relatively low absorption cross section. The upper half of the capsule is bolted to the lower half using four socket head cap screws. A threaded hole in the upper half supports a set screw that is used to supply the clamping pressure to the beam which measures 23.7 x 2.0 x 0.554 mm (L x W x T) with a cantilevered length of 16.8 mm. Two 1/16 in. diameter holes in the upper half are used to position the optical fiber probes over the base and tip of the cantilever beam. The probes are held in position using set screws that thread into the side of the capsule. An additional hole allows a thermocouple to be positioned in the capsule, adjacent to the beam. A threaded hole in the center of the upper half is used to attach the capsule to the support rod.

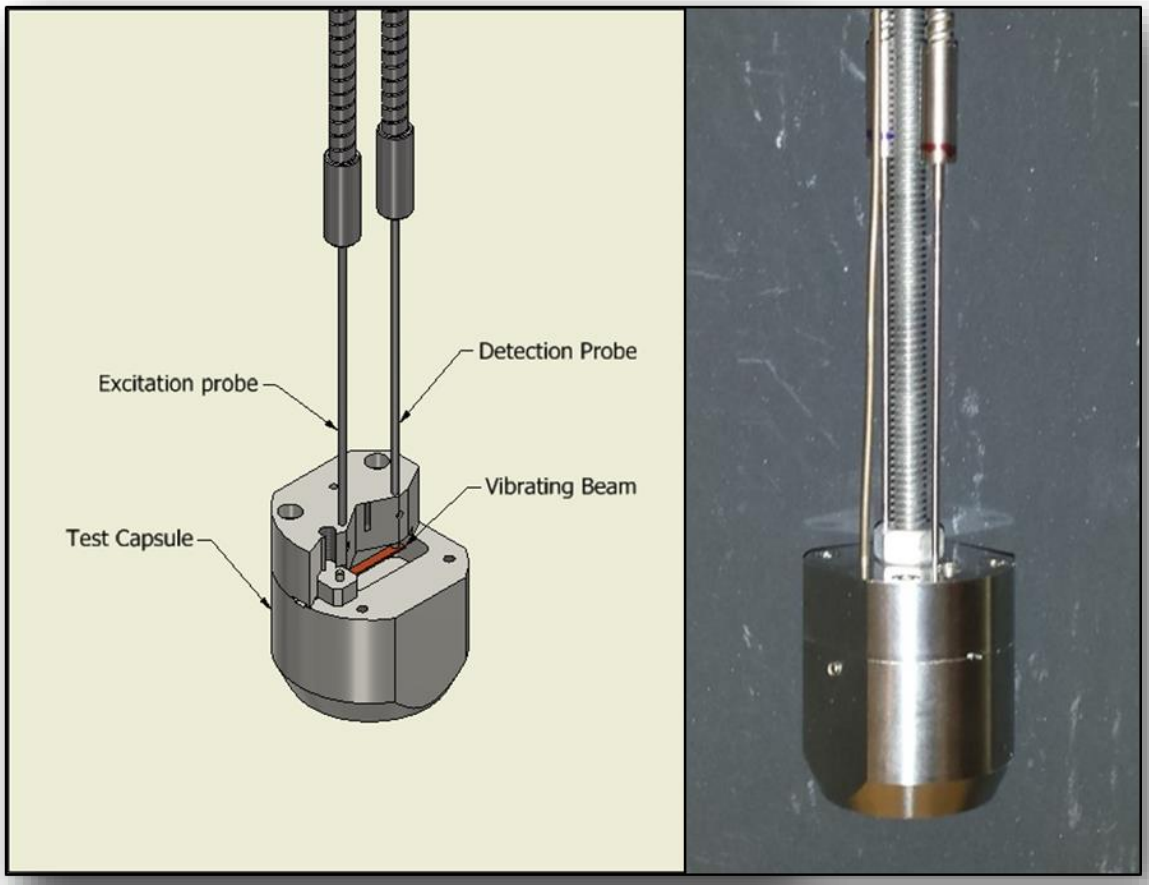

Figure 1. Section view of the test capsule showing the cantilever beam with excitation and detection probes (left), capsule prior to reactor test (right).

3. DEPLOYMENT AND TEST RESULTS

3.1 Deployment

An irradiation test of the device, named RUSL, was planned for spring of 2019 at the TREAT reactor. The TREAT reactor is part of the Materials and Fuels Complex (MFC) at INL. It is an air-cooled, thermal-spectrum reactor that provides transient testing of nuclear fuels and materials. It has an open-core design that allows simplified access for experiment instrumentation. The planned irradiation called for the capsule to be incorporated into the Broad Use Specimen Transient Experiment Rig (BUSTER) for insertion in the reactor. BUSTER is a pre-qualified, reusable test module used to house experiments for radiation in TREAT. BUSTER provides primary and secondary containment and contains a heating module for controlled temperature experiments. A prototype instrument capsule was delivered to the TREAT facility in late April 2019. The prototype was inserted into BUSTER to allow testing and calibration of the heater outside the reactor before the actual test. It was determined that rather than a short high flux transient, the reactor would be run in steady state mode at 80 kW. This would allow the sample to be held at a constant temperature during irradiation to better identify the effects of irradiation on the recrystallization process. The instrument capsule along with the laser, detection light source and

ancillary equipment were delivered to the reactor in early May 2019. The equipment was setup in the experimenter's room at the TREAT facility. Optical fibers and a thermocouple wire were run from the experimenter's room to the top of the reactor where they could be connected to the instrument capsule leads. The instrument capsule was loaded into BUSTER and inserted into the reactor on May 9, 2019. Initial tests were run to verify proper operation. Figure 2 is a composite photo of the RUSL device in the staging area and its transport and insertion into the TREAT reactor.

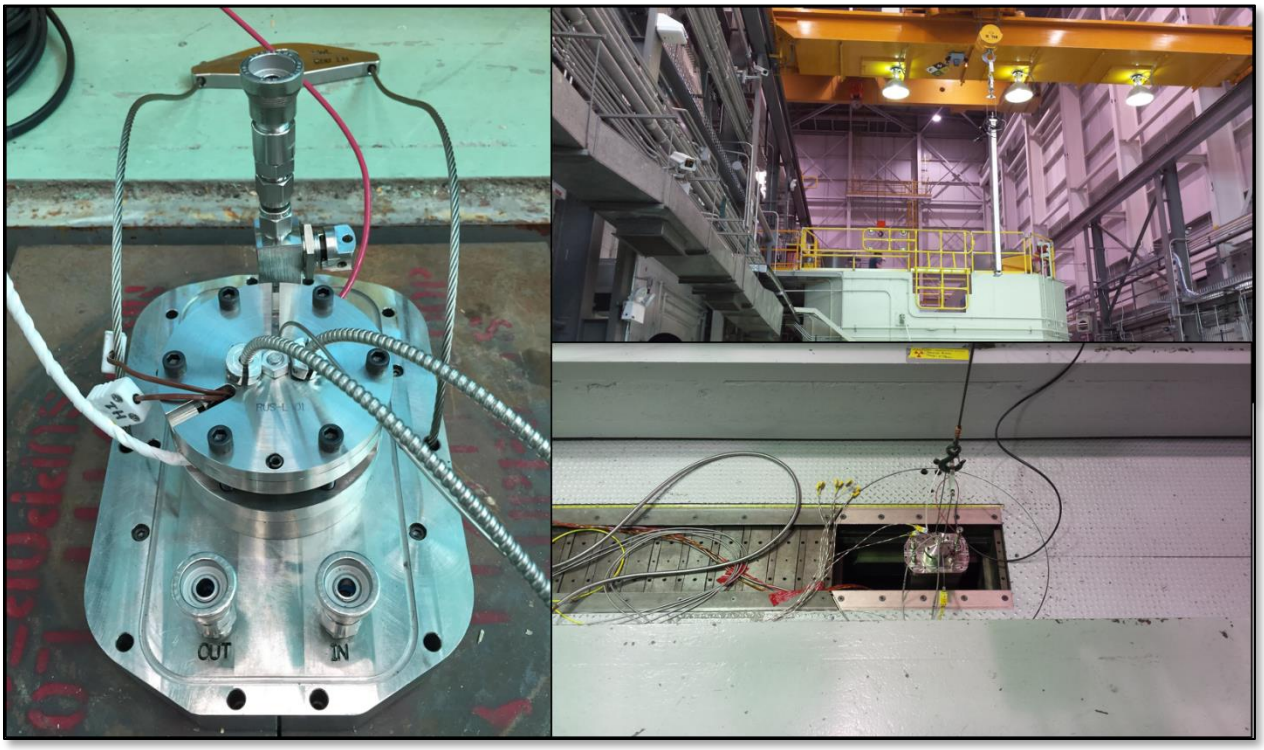

Figure 2. RUSL deployment in the TREAT reactor. RUSL in BUSTER at the staging area (LH), transport to the reactor (upper RH), lowering into the test position (lower RH).

3.2 Irradiation Testing

The capsule irradiation test, named MIMIC-RUSL, was conducted on May 13, 2019. Pretests of the data collection were run to verify proper operation and the data collection was started at 9:47 am with frequency scans approximately every 45 seconds. After the required briefings, the reactor went critical at about 10:15 am and reached the steady state test power of 80 kW at about 10:47 am. The experiment heater was turned on shortly thereafter and reached 159.7°C at 11:50 am. At this point the temperature controller was cycled off and on to minimize temperature overshoot. This caused the temperature to drop to 156.7°C at 12:05 pm and then gradually increase to the set point of 160°C. The temperature was held near the set point until 2:47 pm at which point the reactor was shut down. The capsule temperature was then raised to 230°C over the course of the next hour to ensure complete recrystallization of the sample. The experiment heater was then turned off and the capsule was allowed to naturally cool. At about 4:30 pm the scan spacing was changed to once every 5 minutes and data continued to be collected over night until 9:10am on the morning of May 14, 2019. At this point the experiment had cooled to 28.5°C. A series of post irradiation scans were run to explore higher flexural modes and the data collection was turned off. A plot of the experiment temperature vs time is presented in Figure 3.

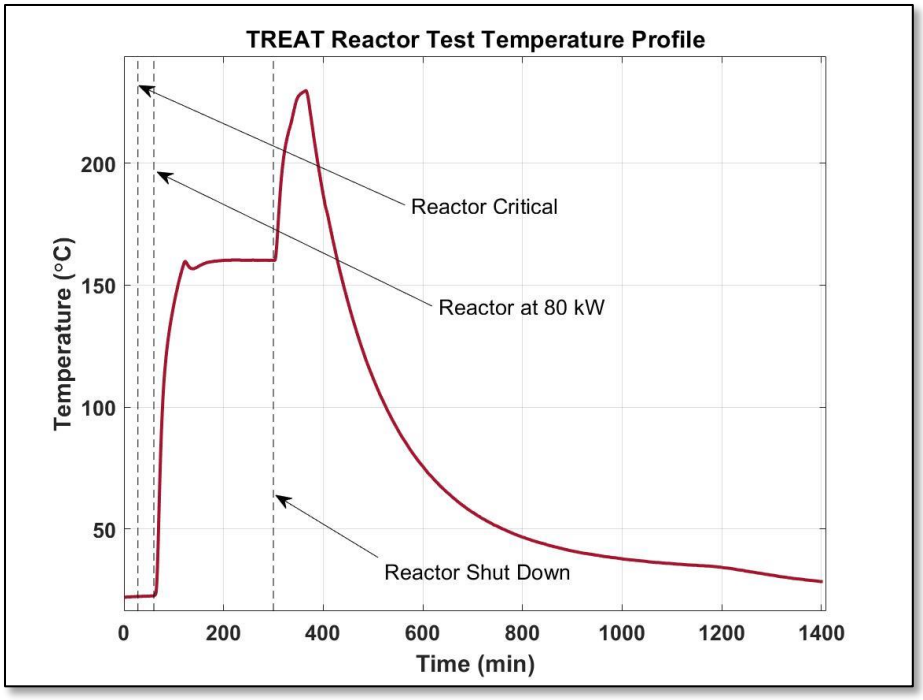

Figure 3. Irradiation test temperature profile.

3.3 Irradiation Test Results

The results of the irradiation test are presented in this section and compared to results obtained in tests conducted in the laboratory. Figure 4 shows the signal amplitude vs the excitation frequency as the frequency is scanned through the beam resonance. As the sample undergoes grain restructuring, the resulting change in the modulus of elasticity causes a change in the resonant frequency of the beam vibration. This change is clearly seen in the figure which shows the first and last frequency scans of the test. The resonant peak is observed to shift from 1188 Hz prior to grain restructuring to 921 Hz after grain restructuring. Figure 5 is a plot of the resonant frequency for the duration of the test vs the temperature. Initially the resonant peak declines gradually in a linear fashion due to the change in modulus with temperature. Once recrystallization begins the modulus changes rapidly at constant temperature. The rate and extent of the recrystallization depend on both temperature and time. Tests conducted in the lab showed that for the highly textured copper material used in the experiment recrystallization completed in around 10 minutes at 230°C. At 150°C the process stabilized only after about 3 hours and then required higher temperatures to complete the process. A target temperature of 160°C was set for the irradiation test. This allowed a stable extent of completion to be attained in approximately two hours. After this two hour period the sample was heated rapidly to 230°C to complete the recrystallization process. The recrystallization process is clearly seen in the figure as the resonant frequency drops as the temperature is held at 160°C. The elastic modulus and thus the resonant frequency drops slightly more as the experiment is heated to 230°C and then the resonant frequency decreases linearly as the sample is cooled back to ambient temperature.

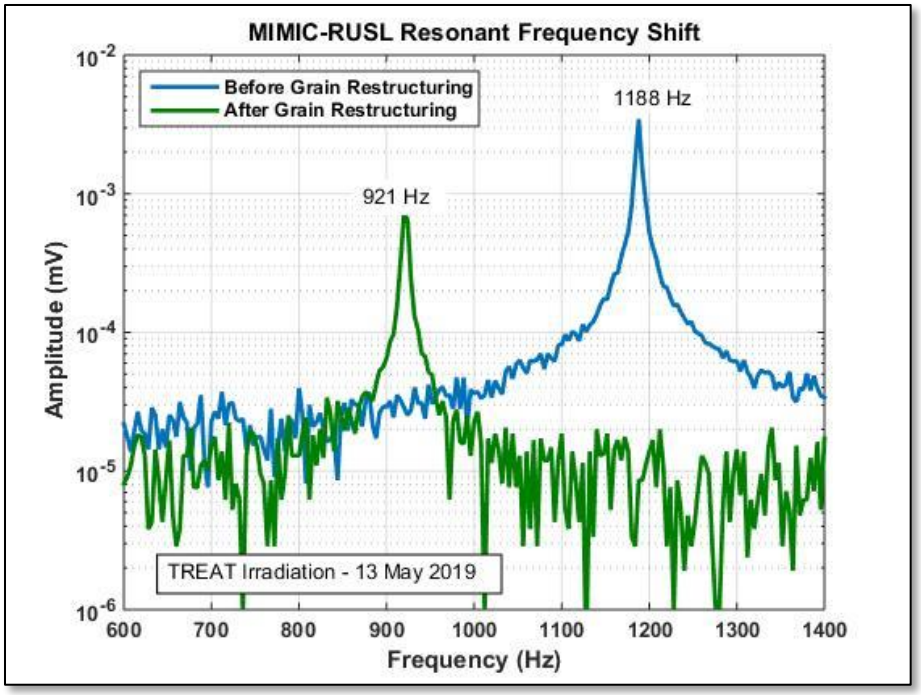

Figure 4. Frequency scans of beam vibrations before and after grain restructuring

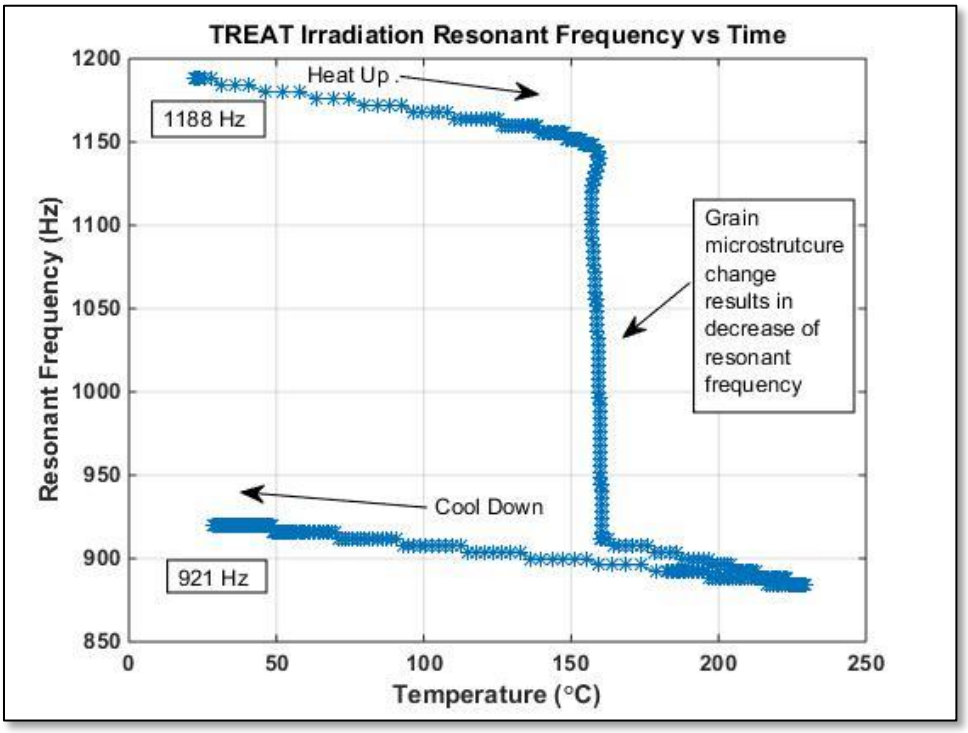

Figure 5. Resonant frequency shift resulting from recrystallization.

The results presented demonstrate the ability to measure a microstructural change through its impact on the elastic modulus of the material during irradiation. To assess the effect of radiation on the recrystallization process the results of the irradiation test were compared to a test run in the laboratory. As mentioned the recrystallization process is a function of time and temperature. To isolate the radiation impact, heating profiles of the irradiated and un-irradiated tests would ideally be identical. The heating profiles of the two tests are shown in Figure 6. Since the heating profiles are not identical, the x-axis or time was matched when the temperatures were both 150°C. This was done since the process occurs much more slowly at lower temperatures so by aligning the data at 150°C the data could be more accurately compared. Figure 7 shows a comparison of the resonant frequency vs temperature. The data sets are very similar although it is noted that the temperature of the IRC test was slightly higher than the TREAT test. The resonant frequencies at the start and end of the both tests were almost identical. The before and after frequencies for IRC test were 1,190 Hz and 924 Hz respectively and 1,188 Hz and 921 Hz for the TREAT test. Figure 8 shows a comparison of the resonant frequencies vs time for each of the tests. The x-axis was again adjusted so that the time was equal when the temperature reached 150°C. The curves are very similar except that the resonant frequency dropped slightly faster in the IRC test. This is to be expected since as seen in figure 7 the temperature in the IRC test was slightly higher. The conclusion to be drawn is that for the low irradiation rate and total dose, the radiation had negligible effect on the recrystallization rate. As discussed in the next section, this was to be expected.

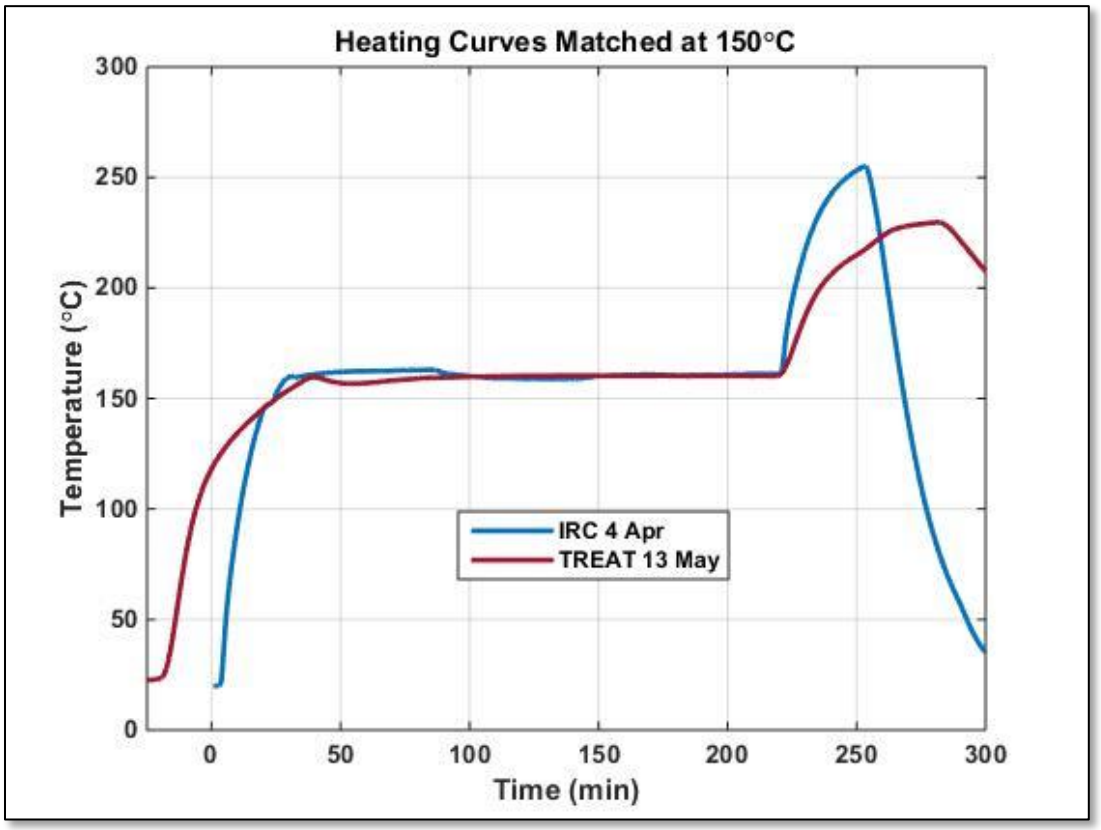

Figure 6. Temperature profile - IRC vs TREAT

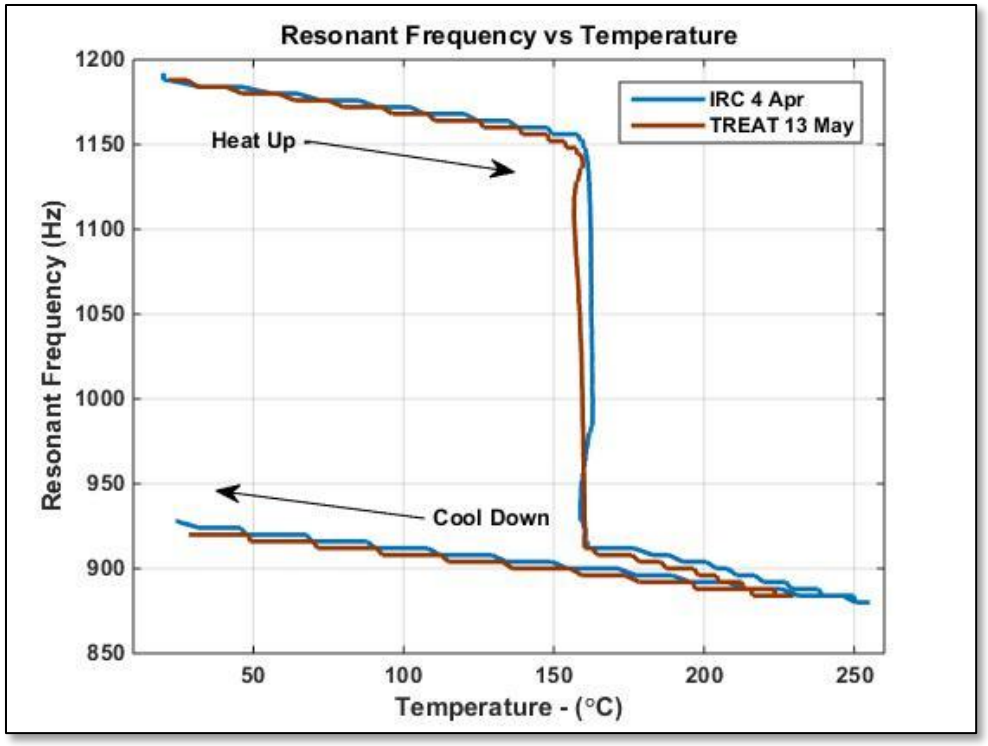

Figure 7. Resonant frequency vs temperature - IRC vs TREAT

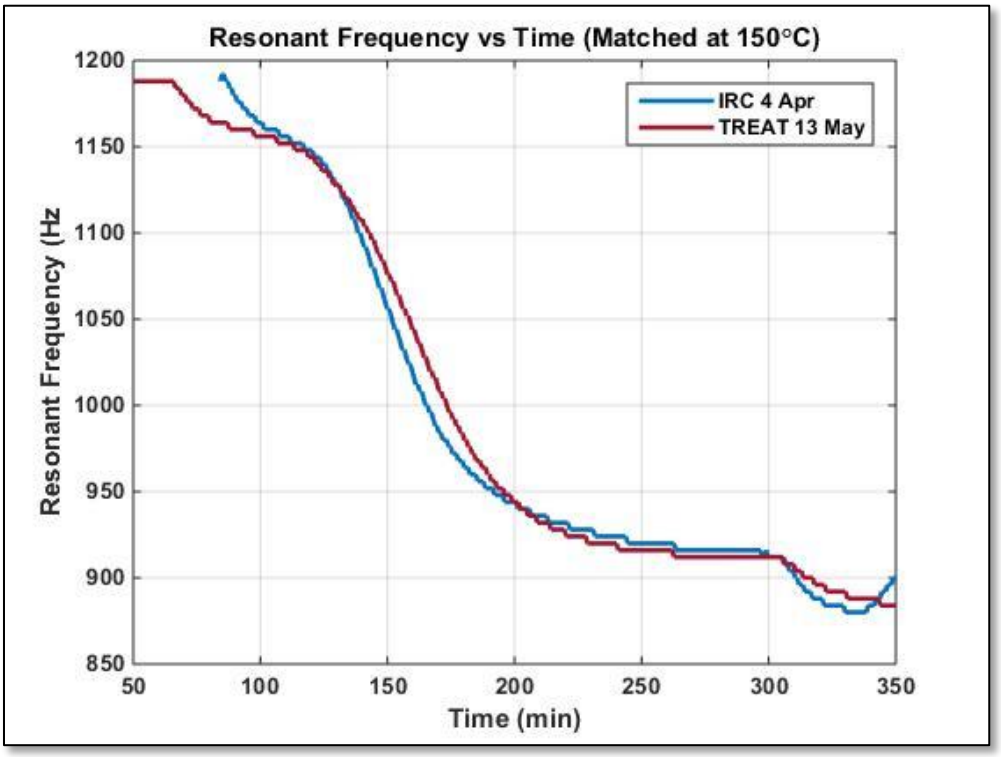

Figure 8. Resonant frequency vs time - IRC vs TREAT

4. RADIATION EFFECTS SCOPING STUDY

4.1 Feasibility Study Calculations

As a first step in conducting a feasibility study of the ability to induce radiation effects, we make use of a previous investigation that looked at the influence of ion irradiation on an fcc metal alloy. While these results are not directly transferable to the current study involving a pure copper sample, they do help identify the experimental parameters that govern radiation assisted recrystallization. The key material parameters are the barrier to dislocation motion and the starting dislocation density and the key reactor parameters are neutron flux and spectrum. The material parameters we use in this study are from a previous investigation involving a copper alloy and the reactor parameters correspond to steady state operation of the TREAT reactor and the centerline position in the neutron radiography reactor (NRAD). It is noted here that while realistic numbers for damage accumulation in the copper for both TREAT and NRAD irradiation was obtained using the Monte Carlo N-Particle (MCNP), the material parameters used are for a copper alloy and give results that can't be compared to what one would expect for pure copper. The next step for the feasibility study will be to use more represented numbers for the dislocation density and a better estimate for the barrier to dislocation motion.

In past experiments by Zinkle et al., irradiation has been observed to reduce the temperature required for recrystallization to occur in copper alloys [16]. Zinkle and co-authors hypothesized that the reason for this reduction was due to the enhanced concentration of vacancy and interstitial defect species, leading to an increase in the self-diffusion coefficient of copper atoms under irradiation.

To determine if a similar reduction of recrystallization temperature would occur under irradiation in INL's TREAT or NRAD reactors, a similar approach to Ref. 16 was used. A brief summary of this approach follows; for further details, please see Ref. 16 and 17. In the absence of irradiation, the self-diffusion coefficient of copper atoms D_{SD} is given by by

$$D_{SD} = D_v X_v^{eq}$$

where D_v is the vacancy diffusion coefficient and X_v^{eq} is the equilibrium atomic fraction of vacancies. In the presence of irradiation, the self-diffusion coefficient of copper atoms is increased due to the increased steady-state vacancy concentration. This can be calculated as follows:

$$D_{rad} = D_v(X_v^{eq} + X_v^{ss})$$

where D_{rad} is the radiation-enhanced self-diffusion coefficient and X_v^{ss} is the steady-state concentration of vacancies caused by irradiation. X_v^{ss} is calculated using Equation 5.14 in Ref. 17, with material properties described in Ref. 16.

For the INL reactors, the source term strength K_0 that appears in Equation 5.14 was calculated as follows. Using the MCNP code, the damage rate K in dpa/s was calculated as a function of power for the TREAT and NRAD reactors. The source strength was then calculated using $K_0 = K\eta$ where $\eta = 0.15$ is the cascade survival fraction (fraction of Frenkel pairs that survive the immediate collision cascade) for copper.

Based on these calculations, the self-diffusion coefficients in equilibrium (thermal) conditions and under irradiation were plotted as a function of temperature. (Figure 3 in Ref. 16 was reproduced using the source strength given in the paper to verify the Matlab code used to determine the diffusion coefficients.) The diffusion coefficient versus temperature plots were used to determine whether recrystallization is predicted to be enhanced for a given experiment, as further described in the following sections.

4.2 Feasibility in TREAT

For TREAT, two different scenarios were considered based on power limitations. According to MCNP calculations, TREAT can produce a damage rate K of 1.83×10^{-9} dpa/s per MW of power, or 1.83×10^{-9} dpa/s/MW. TREAT can operate for a 10-hour period at 100 kW, resulting in $K_0 = 2.75 \times 10^{-11}$ dpa/s. The irradiation-enhanced diffusion coefficient at this power is shown in Figure 9(a).

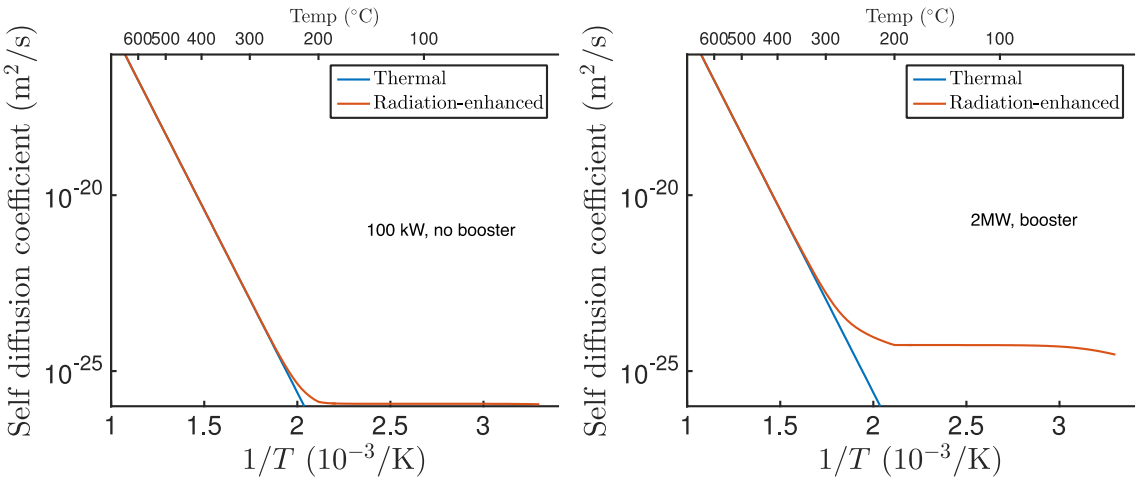

Figure 9. (a) Radiation-enhanced self-diffusion coefficient of copper in TREAT, at 100 kW power. (b) Radiation-enhanced self-diffusion coefficient of copper in TREAT with uranium booster at 2MW power.

As seen in Fig. 9(a), the radiation-enhanced diffusion coefficient begins to deviate from the thermal diffusion coefficient when T < 260°C, meaning there will be no radiation-enhanced reduction in recrystallization temperature unless T < 260°C. At this temperature, recrystallization time in the absence of irradiation is expected to be > 10 years [18]. Because this is much longer than the 10-hour time frame for the experiment to be conducted, no radiation-enhanced reduction in recrystallization temperature is predicted to be observed.

The other scenario considered for TREAT was for a shorter operation time of 1000 seconds at the maximum allowable power during transient operation of 2 MW. The damage level was also boosted by placing a thin U sample in contact with the Cu sample. In this scenario, the source strength was $K_0 = 1.83 \times 10^{-9}$ dpa/s. The corresponding radiation-enhanced diffusion coefficient is plotted in Figure 9(b). In this scenario, the radiation-enhanced diffusion coefficient begins to deviate from the thermal diffusion coefficient when T < 300°C. However, at this temperature, recrystallization time in the absence of irradiation is still expected to be > 10 years [18], so no radiation-enhanced reduction in recrystallization temperature is predicted to be observed during the 1000 second maximum duration of the experiment at this power.

4.3 Feasibility in NRAD

In the NRAD reactor, maximum power is 0.25 MW for a time of up to 8 days. MCNP calculations for the dry tube at the centerline position showed that the predicted damage rate K was 2.68×10^{-9} dpa/s/MW, resulting in a source strength of $K_0 = 1.0 \times 10^{-10}$ dpa/s. The resulting radiation-enhanced diffusion coefficient is shown in Figure 10.

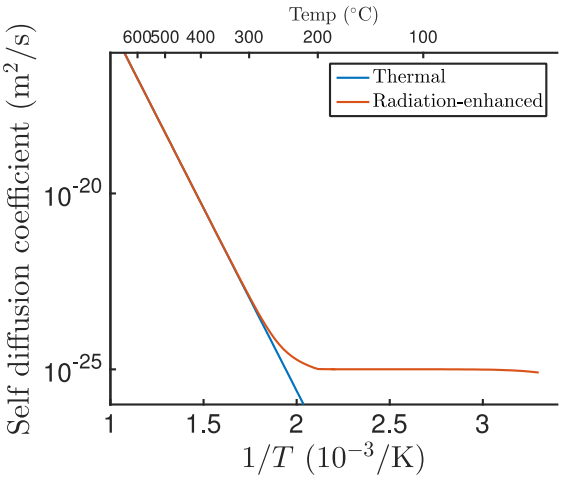

Figure 10. Radiation-enhanced self-diffusion coefficient of copper in NRAD at 0.25 MW power.

As seen in Figure 10, the radiation-enhanced diffusion coefficient begins to deviate from the thermal diffusion coefficient when T < 290°C. However, at this temperature, recrystallization time in the absence of irradiation is still expected to be > 10 years [18], so no radiation-enhanced reduction in recrystallization temperature is predicted to be observed during the 8 day maximum duration of the experiment at this power.

5. SUMMARY

Grain restructuring or recrystallization occurs in both metal and ceramic nuclear fuels during irradiation and can result in dramatic changes in properties. Measurement of elastic properties can be tied directly to these changes in microstructure. In this report, we have described the methodology and design of an instrument used to monitor microstructural changes of a copper sample with a highly textured grain microstructure during irradiation. The approach involves monitoring the resonant frequency of a thin cantilever beam using optical methods for excitation and detection. The instrument capsule was deployed in the TREAT reactor and an irradiation test was performed in May 2019. The results of the experiment confirmed the ability to measure the recrystallization of the copper under irradiation. Analysis of the data showed negligible radiation impact. Scoping studies were conducted to determine if radiation doses during either a transient at the TREAT reactor or irradiation at the NRAD reactor would impact the recrystallization process. The scoping are still in progress and the next step will involve using material parameters associated with a highly textured pure copper sample.

6. REFERENCES

[1] S. Hu, V. Joshi, C. A. Lavender, "A Rate-Theory-Phase-Field Model of Irradiation-Induced Recrystallization in UMo Nuclear Fuels," *JOM* **69**(12), pp. 2554-2562 (2017).

[2] P.G. Lucuta, R.A. Verrall, Hj. Matzke, B. J. Palmer, "Microstructural Features of SIMFUEL – Simulated High-Burnup UO2-based Nuclear Fuel," *J. Nuc. Mat*., **178**, pp. 48-60 (1991).

[3] V. Vincenzo, t. Wiss. "The high burn-up structure in nuclear fuels," *Mater. Today*, **13** (12), pp. 24-32 (2010).

[4] Gatt, J.-M., et al. "Elastic behavior of porous ceramics: application to nuclear fuel materials." Journal of Nuclear Materials 336.2-3 (2005), 145-155.

[5] K. Hattar, D.C. Bufford, D.L. Buller, "Concurrent in situ ion irradiation transmission electron microscope," Nucl. Instr. Meth. Phys. Res. B 338 (2014) 56-65.

[6] R. S. Schley, D. H. Hurley, Z. Hua, "Optical fiber technique for in-reactor mechanical properties measurement," *AIP Conference Proceedings*, Denver, CO, 15-20 July 2012, **1511**, pp. 1701-1709 (2013).

[7] ASTM E1875-08, ASTM International, West Conshohocken, PA, 2008.

[8] ASTM C747-93, ASTM International, West Conshohocken, PA, 1993.

[9] ASTM C623-92, *ASTM International*, West Conshohocken, PA, 1992.

[10] S. P. Timoshenko, *History of Strength of Materials*, Dover, New York, 1953.

[11] J. W. Strutt, Theory of Sound, Macmillan, London, 1877.

[12] S.M. Han, H. Benaroya, T. Wei, "Dynamics of Transversely Vibrating Beams Using Four Engineering Theories," J. of Sound and Vibration, 225(5), 935-988, (1999).

[13] K. F .Graff, Wave Motion in Elastic Solids, Dover, New York, 1991, p. 157.

[14] I. G. Ritchie, "Improved Resonant Bar Techniques for the Measurement of Dynamic Elastic Moduli and a Test of the Timoshenko Beam Theory," *J. of Sound and Vibration*, **31**(4), 453-468, (1973).

[15] R. O. Cook, C. W. Hamm, "Fiber optic lever displacement transducer," *Applied Optics*, **18**(19), 3230-3241, (1979).

[16] S. J. Zinkle, G. L. Kulcinski, L. K. Mansur, *Journal of Nuclear Materials*, v. 141-143, p. 188-192 (1986).

[17] G. S. Was, *Fundamentals of Radiation Materials Science*, Springer (Berlin), 2007.

[18] S. J. Zinkle, D. H. Plantz, A. E. Bair, R. A. Dodd, G. L. Kulcinski, *Journal of Nuclear Materials*, v. 133&134, p. 685-689 (1985).